A New Approach to the Design of Dual-Mode Rectangular Waveguide Filters with Distributed Coupling

Patrizia Savi, Daniele Trinchero, Riccardo Tascone, and Renato Orta, *Member, IEEE*

***Abstract*— A synthesis procedure for a new configuration of four-pole dual-mode waveguide filters with distributed coupling is presented. In this configuration the dual-mode coupling is obtained by exploiting the well-known fact that the diagonal polarizations are coupled in an almost square waveguide. The obvious advantage of this type of structure is that the cross sections of all the discontinuities are rectangular, hence the global prediction of the filter is more accurate. The synthesis approach is based on a scattering matrix formulation where the dual-mode coupling is described in terms of a 2×2 propagation matrix. Universal design charts, which directly yield the scattering parameters of the various junctions, have been obtained. Comparisons with experimental results of a four-pole filter are also presented.**

***Index Terms*— Bandpass filters, cavity resonator filters, distributed parameter filters, equipipple filters, microwave filters, rectangular waveguides, waveguide filters.**

I. Introduction

As IS well known, the use of dual-mode cavities allows the realization of compact high-quality microwave filters and multiplexers [1]. The dual-mode coupling is obtained conventionally by means of tuning screws [2]–[4]. In order to eliminate the need of experimental tuning, efforts have been made to replace tuning screws with suitable discontinuities [5], [6]–[7]. An alternative technique exploits the possibility of coupling the modes for the whole cavity length by means of corner cuts in square or rectangular waveguides [8], [9]. This solution can provide advantages in terms of power handling capability, production cost, and compactness (dielectric-filled cavities can be considered). In this case, the resonators have a uniform cross section quite close to that of the waveguide without cuts since the coupling is distributed, but even if the cross-section perturbation is small, the mode spectrum must be computed numerically. Therefore, if a high precision is required (as in the case of narrow-band filters) this step can be cumbersome.

The configuration we have proposed in [10] definitely overcomes this problem. In fact, the resonators consist of an almost square waveguide and the dual-mode coupling occurs between the diagonal modes of the square waveguide. In other words, the usual TE_{10} and TE_{01} modes are viewed as sum and difference modes, in the context of the coupled mode theory [11]. Of course, in this configuration the rectangular thick slots that realize the input/output and intercavity coupling are rotated by 45° with respect to the cavity cross section. The obvious advantages of this type of filter, which allow an easier prediction, are that the distributed coupling is evaluated in closed form and that the cross section of all discontinuities have a rectangular shape.

Dual-mode filters are generally designed on the basis of a lumped circuit prototype. When the coupling is realized by means of coupling screws, the final response of the filter is then obtained by means of experimental tuning. In the case of distributed coupling configurations, starting from the study of the dual-mode coupling on the basis of which the initial dimension of the filter are determined, the final configuration is generally obtained by means of a computer-aided optimization process.

In this paper we present a new synthesis procedure based on a scattering matrix characterization of the various coupling discontinuities. First, a distributed modal circuit of the filter is introduced and discussed. Then, starting from this circuit, the synthesis procedure which exploits the properties of the scattering matrix of reciprocal and lossless devices is presented. For clarity, in Section II a dual-mode cavity is investigated. Then, on the basis of the concepts introduced in this simpler case, Section III deals with a synthesis procedure of four-pole dual-mode filters. The synthesis scheme was condensed in three design charts that directly yield the scattering parameters of the various coupling discontinuities in terms of the filter response specifications. The synthesis directly gives the final dimensions of the filter and no optimization is required. This result is due to the fact that the design is directly based on this distributed model and is, therefore, much closer to the physical behavior of the filter. Comparisons among design curve, full-wave analysis, and measurements on a breadboard confirm the validity of the approach.

Dual-mode elliptic function filters can be obtained with this configuration, as confirmed by the full-wave analysis.

II. Dual-Mode Cavity

Before presenting the design procedure we have developed for dual-mode two-cavity filters, it is beneficial to consider the simpler case of a single dual-mode cavity. The cavity consists of a length of an almost square waveguide and the input/output

Manuscript received December 12, 1995; revised October 18, 1996.

The authors are with CESPA (CNR), Dipartimento di Elettronica, Politecnico di Torino, 10129 Torino, Italy (e-mail: savi@polito.it).

Publisher Item Identifier S 0018-9480(97)00826-0.

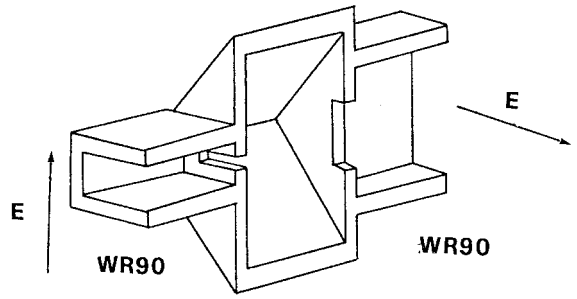

Fig. 1. Cutaway perspective of the proposed dual-mode cavity.

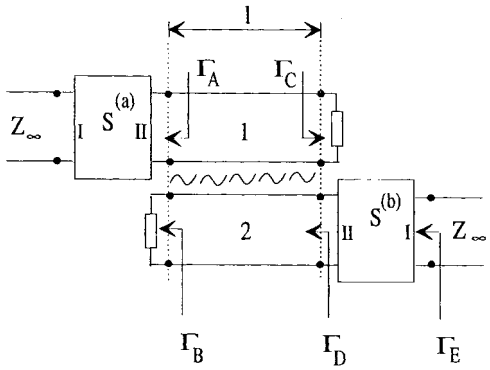

Fig. 2. Modal circuit of the dual-mode single cavity filter. The transmission lines of length l refer to the diagonal modes of the unperturbed waveguide. The modal coupling is symbolically indicated by a wavy line.

couplings are obtained by two thick rectangular slots rotated by 45° with respect to the sides of the cavity cross section (see Fig. 1). Clearly, the two slots are perpendicular to each other in such a way that a dual-mode response is obtained. The almost square waveguide, with sides a and b, can be seen as a perturbation of the square waveguide with side $a_s = (a+b)/2$ (hereinafter called unperturbed guide). From this point of view, we could say that each slot couples the TE_{10} mode of the input/output waveguide with one of the two diagonal modes of the unperturbed guide. These last two modes are the sum and the difference of the degenerate TE_{10} and TE_{01} modes of the unperturbed guide. Due to the perturbation introduced (the cross section of the cavity is not exactly square), these two diagonal modes are coupled to each other for the whole length of the cavity. In other words, we realize a distributed coupling between the diagonal modes of the unperturbed waveguide by simply using a rectangular cross section.

Slightly perturbed guides are generally studied by means of the coupled mode theory [11], according to which the characteristics of the relevant modes can be obtained. For this configuration, this study is not necessary at all, because we already know the relevant modes of the coupled structure (which are the well-known TE_{10} and TE_{01} modes of the almost square waveguide). Thus, the dual-mode coupling is known in closed form, and it can be controlled analytically by varying the difference of the side lengths of the cavity cross section. Notice that a slight difference (about 1%) is generally required because the dual-mode coupling occurs for the whole length of the cavity.

Some readers could find another interpretation more attractive, according to which the first slot excites equally the TE_{10} and TE_{01} modes of the unperturbed waveguide, while the second slot is decoupled because it excites them with opposite sign. If we now introduce a slight difference between the side lengths of the cavity cross section, the propagation constants of these two modes change giving rise to a rotation of the field polarization so that coupling occurs through the second slot. Even if this interpretation could look more straightforward, it is not convenient from a design point of view. In fact, it requires the use of 3×3 scattering matrices to describe the discontinuities, whereas, according to the first interpretation, where the slots couple only one of the diagonal modes, only 2×2 scattering matrices are involved.

Following the description in terms of coupled diagonal modes, the modal circuit of a single dual-mode cavity filter is shown in Fig. 2. The two transmission lines of length l corresponds to the two diagonal modes of the unperturbed waveguide (1, 2) and the distributed coupling is symbolically sketched by a wavy line. The 2×2 scattering matrices $\mathbf{S}^{(a)}$ and $\mathbf{S}^{(b)}$ refer to the discontinuities between the cavity and the external waveguides at the input and output sections, respectively. The two ports of these scattering matrices refer to the TE_{10} mode of the input/output waveguide and to one of the two diagonal modes of the cavity. At the same section, the other diagonal mode is reactively loaded because it is coupled through the slot with the TE_{01} mode of the external waveguide which is evanescent. In Fig. 2 these reactive loads are represented by the reflection coefficients Γ_B and Γ_C corresponding to the diagonal modes 2 and 1, respectively.

Because of the distributed modal coupling, the propagation operator $\mathbf{P}$, in the diagonal mode basis, is given by the matrix

$$\mathbf{P} = e^{-j\theta}\begin{bmatrix} \cos(\Delta\theta/2) & j\sin(\Delta\theta/2) \\ j\sin(\Delta\theta/2) & \cos(\Delta\theta/2) \end{bmatrix} \tag{1}$$

where

$$\Delta\theta = \theta_{TE_{10}} - \theta_{TE_{01}} \sim \pi\left(\frac{l}{a_s}\right)^2 \left(\frac{\Delta a}{a_s}\right)\frac{\pi}{\theta} \tag{2}$$

is the electrical length difference between the two relevant modes of the cavity (i.e., the usual TE_{10} and TE_{01} modes) which, in the light of the coupled mode theory, is interpreted as the coupling coefficient; θ is the cavity electrical length for the modes in the unperturbed waveguide, and $\Delta a = a - b$. Using (1), the reflection coefficient Γ_D of Fig. 2 can be expressed as a function of θ in the following way:

$$\Gamma_\mathrm{D}(\theta) = e^{-2j\theta}\frac{\Gamma_\mathrm{B}\cos^2(\Delta\theta/2) - \Gamma_\mathrm{A}\sin^2(\Delta\theta/2)] - \Gamma_\mathrm{A}\Gamma_\mathrm{B}\Gamma_\mathrm{C}\, e^{-2j\theta}}{1 - \Gamma_\mathrm{C}\left[\Gamma_\mathrm{A}\cos^2(\Delta\theta/2) - \Gamma_\mathrm{B}\sin^2(\Delta\theta/2)\right] e^{-2j\theta}} \tag{3}$$

where, for clarity, we have denoted the scattering parameter $S_{22}^{(a)}$ with Γ_A. It can be shown that for small values of $\Delta\theta$ and of the phase difference $(\phi_\mathrm{B} - \phi_\mathrm{A})$ between the reflection coefficients Γ_B and Γ_A (which is actually the case occurring in practice), the following symmetry condition holds:

$$\Gamma_\mathrm{D}(\theta_0 - \theta) \sim \Gamma_\mathrm{D}^*(\theta_0 + \theta)\, e^{-2j(\phi_\mathrm{A} - \phi_\mathrm{B} + \phi_\mathrm{C})} \tag{4}$$

where

$$\theta_0 = (\phi_\mathrm{A} + \phi_\mathrm{C})/2. \tag{5}$$

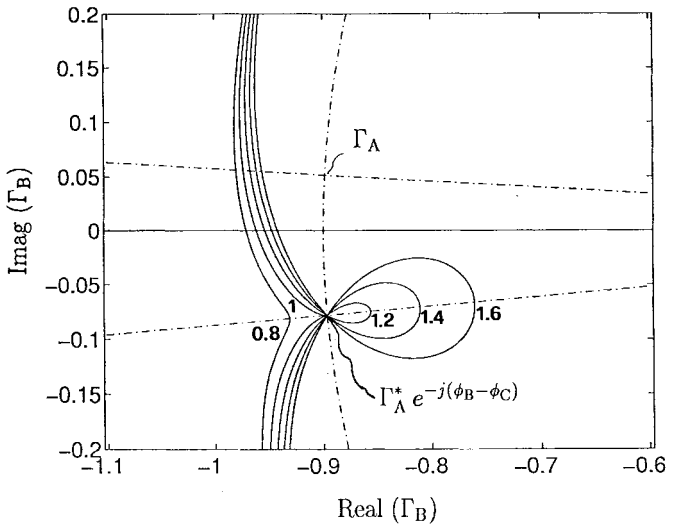

Fig. 3. Example of $\Gamma_D(\theta)$ curves for different values of the distributed coupling parameter $\Delta\theta/\Delta\theta_c = [0.8, 1, 1.2, 1.4, 1.6]$.

Equation (4) means that symmetric values of θ with respect to θ_0 correspond to points of the Γ_D plane symmetric with respect to the radial line through $\Gamma_A^* \exp[j(\phi_B - \phi_C)]$. Plots of $\Gamma_D(\theta)$ for different values of the parameter $\Delta\theta$ are shown in Fig. 3. Two coupling states can be identified, according to whether $\Delta\theta$ is larger or smaller than a critical value $\Delta\theta_c$ given by

$$\sin(\Delta\theta_c/2) = (1 - |\Gamma_A|)/(1 + |\Gamma_A|). \tag{6}$$

If $\Delta\theta > \Delta\theta_c$ (over-coupling state) the curve of $\Gamma_D(\theta)$ has a double point at $\Gamma_D = \Gamma_A^* \exp[j(\phi_B - \phi_C)]$; this means that this last value is reached for $\theta = \theta_{d1}, \theta_{d2}$ such that

$$\cos\left(\frac{\theta_{d1} - \theta_{d2}}{2}\right) = \frac{\cos(\Delta\theta/2)}{\cos(\Delta\theta_c/2)}. \tag{7}$$

For $\Delta\theta < \Delta\theta_c$ (under-coupling state) the right-hand side (RHS) of (7) is greater than one and the double point occurs for imaginary values of θ. However, in both cases, for real θ values, the curve has a minimum of $|\Gamma_D|$ for $\theta = \theta_0$ given by

$$|\Gamma_D|_{min} = \left|\frac{[1 - \sin^2(\Delta\theta/2)] - |\Gamma_A|[1 + \sin^2(\Delta\theta/2)]}{[1 + \sin^2(\Delta\theta/2)] - |\Gamma_A|[1 - \sin^2(\Delta\theta/2)]}\right|. \tag{8}$$

This minimum value is less than $|\Gamma_A|$ in the over-coupling state whereas the converse is true in the under-coupling state.

If we assume the input/output discontinuities to be reciprocal and lossless, the magnitude of the input reflection coefficient Γ_E can be written as follows:

$$|\Gamma_E| = |S_{22}^{(b)*} - \Gamma_D|/|1 - \Gamma_D S_{22}^{(b)}|. \tag{9}$$

Hence, it is obvious that if the two discontinuities are identical, and in particular $S_{22}^{(b)} = \Gamma_A$ and $\Gamma_C = \Gamma_B$, the double point in the curve $\Gamma_D(\theta)$ gives rise to two reflection zeros at θ_{d1}, θ_{d2}. In this condition, a measure of the electrical bandwidth of the filter can be obtained by (7). Furthermore, the input reflection coefficient reaches its maximum value in the passband for $\theta = \theta_0$, given by

$$|\Gamma_E|_{max} = \left|\frac{\sin^2(\Delta\theta/2) - \sin^2(\Delta\theta_c/2)}{\sin^2(\Delta\theta/2) + \sin^2(\Delta\theta_c/2)}\right|. \tag{10}$$

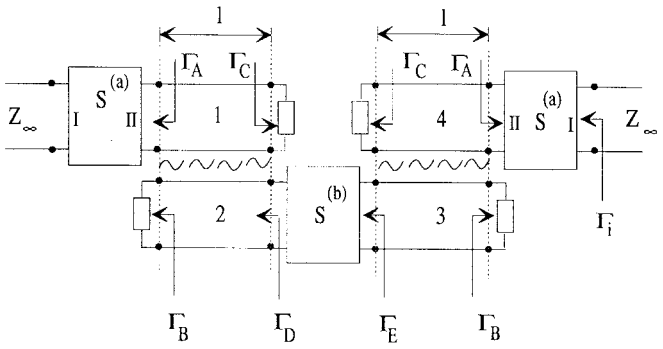

Fig. 4. Modal circuit of a dual-mode two-cavity filter. See the text for the description of the devices.

In other words, the over-coupling state produces a Chebyshev-type response, whereas a Butterworth-type response is obtained when the critical condition $\Delta\theta = \Delta\theta_c$ holds. In the under-coupling state no reflection zeros are obtained because the curve Γ_D does not pass through the point $S_{22}^{(b)*}$.

As far as the Chebyshev response is concerned, the previous equations can be organized to define the design procedure for a single dual-mode cavity filter. Starting from the electrical bandwidth specified through the parameter $C = \cos(\theta_{d1} - \theta_{d2})$ and of the ripple level $S = (1 + |\Gamma_E|_{max})/(1 - |\Gamma_E|_{max})$, we directly obtain the electrical parameters of the filter by the following expressions:

$$\begin{aligned} \sin^2(\Delta\theta_c/2) &= (1 - C)/(2S - C - 1) \\ \sin^2(\Delta\theta/2) &= S\sin^2(\Delta\theta_c/2) \\ |\Gamma_A| &= [1 - \sin(\Delta\theta_c/2)]/[1 + \sin(\Delta\theta_c/2)]. \end{aligned} \tag{11}$$

Once the electrical parameters are determined, the geometry of the cavity is defined by the following relations:

$$l = \frac{\theta_0}{\pi}\frac{\lambda_0/2}{\sqrt{1 - (\lambda_0/2a_s)^2}}, \quad \frac{\Delta a}{a_s} = \frac{\Delta\theta}{\theta_0}\left[\left(\frac{2\,a_s}{\lambda_0}\right)^2 - 1\right] \tag{12}$$

where λ_0 is the free space wavelength at the central frequency and θ_0 is given by (5). Moreover, in the case of narrow-band filters, the effective relative bandwidth B_f is related to the electrical fractional bandwidth B_θ according to the following expression:

$$B_f = B_\theta\left[1 - \lambda_0/(2\,a_s)^2\right]. \tag{13}$$

III. Four-Pole Filter

On the basis of the analysis developed in the previous section, the dual-mode two-cavity configuration can be analyzed considering the modal circuit shown in Fig. 4. Similar to the previous case, each cavity is represented by two transmission lines of length l corresponding to the two diagonal modes (labeled 1, 2 for the first cavity and 3, 4 for the second one). The coupling between the cavities occurs through a thick slot which couples the diagonal modes 2 and 3 (the scattering matrix $\mathbf{S}^{(b)}$ describes this coupling) and loads the other two modes (1 and 4) with a reactive impedance described by the reflection coefficient Γ_C. The input and output couplings are obtained by two identical thick slots described by the

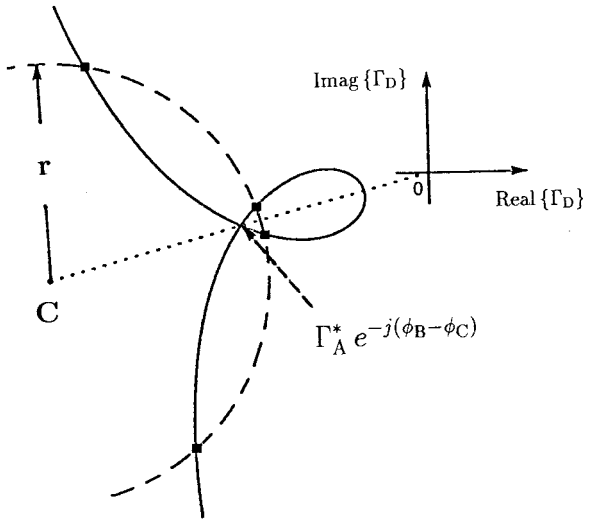

Fig. 5. Example of the curve $\Gamma_{\rm D}(\theta)$ and of the circumference related to the central device in the case of four reflection zeros and $\Delta\theta > \Delta\theta_c$.

scattering matrix $\mathbf{S}^{(a)}$ and by the reactive load $\Gamma_{\rm B}$. Notice that the possibility of controlling the phase $\phi_{\rm B}$ of the reflection coefficient $\Gamma_{\rm B}$ by simply varying the aspect ratio of the slot aperture allows for the tuning of the filter (phase-matching condition) without any further effort.

Our goal is to now obtain the expression of the input reflection coefficient of the filter Γ_i. Recalling that the structure is symmetric, reciprocal, and lossless, the magnitude of this quantity can be simply expressed in terms of the reflection coefficients $\Gamma_{\rm D}$ and $\Gamma_{\rm E}$. In fact, the two-port network described by the scattering matrix $\mathbf{S}^{(b)}$ is loaded on both sides by the same reflection coefficient $\Gamma_{\rm D}$ and presents at its ports the input reflection coefficient $\Gamma_{\rm E}$. Hence, the magnitude of the input reflection coefficient of the filter can be written in the form

$$|\Gamma_i| = |\Gamma_{\rm D}^* - \Gamma_{\rm E}|/|1 - \Gamma_{\rm D}\Gamma_{\rm E}|. \tag{14}$$

Notice that the expression of $\Gamma_{\rm D}$ is still given by (3) and all the considerations previously done still hold. From (14) we can see that the reflection zeros of the filter are related to the condition $\Gamma_{\rm E} = \Gamma_{\rm D}^*$. As is well known, if the central device is symmetric and lossless, the points of the $\Gamma_{\rm D}$ plane transformed by the device in such a way that $\Gamma_{\rm E} = \Gamma_{\rm D}^*$ form a circumference of centre C and radius r given by

$$C = 1/S_{11}^{(b)};\ \ r = |S_{21}^{(b)}/S_{11}^{(b)}|. \tag{15}$$

By these considerations the filter design can be approached geometrically by looking for the intersections of this circumference with the curve $\Gamma_{\rm D}(\theta)$. Fig. 5 shows an example of these intersections for $\Delta\theta > \Delta\theta_c$. This point of view is very convenient for an efficient design procedure because several conditions can be enforced by simple geometrical considerations. In fact, in order to have a symmetric response with respect to the normalized central frequency θ_0, the center of the circumference must be on the symmetry axis of the curve $\Gamma_{\rm D}(\theta)$, as sketched in Fig. 5. From this symmetry condition and (15), the following phase-matching condition is obtained:

$$\angle S_{11}^{(b)} - \phi_{\rm C} = \phi_{\rm A} - \phi_{\rm B}. \tag{16}$$

As far as the magnitude of $S_{11}^{(b)}$ is concerned, we can observe that in order to have four intersections, and hence four reflection zeros in the filter response, the distance

$$d = \sqrt{(1 - |S_{21}^{(b)}|)/(1 + |S_{21}^{(b)}|)} \tag{17}$$

of the circumference from the origin must be greater than the minimum value of $|\Gamma_{\rm D}|$ still given by (8). This yields the condition

$$|S_{11}^{(b)}| > 2\,|\Gamma_{\rm D}|_{min}^2/(1 + |\Gamma_{\rm D}|_{min}^2). \tag{18}$$

The specific value of $|S_{11}^{(b)}|$ can then be determined by requiring the ripple to be a constant in the passband. According to the geometrical interpretation of Fig. 5, the ripple level is related to the distance between that part of the curve $\Gamma_{\rm D}(\theta)$ corresponding to the passband of the filter and the circumference of the central device. Hence, it is easy to observe that low values of the ripple can be obtained if $\Gamma_{\rm D}(\theta)$ has no double point, i.e., if $\Delta\theta < \Delta\theta_c$ (under-coupling state). Furthermore, it can be recognized that:

- the value of the ripple in the passband is a function of the normalized parameter $\Delta\theta/\Delta\theta_c$ only;
- the electrical bandwidth B_θ depends on two parameters: the ratio $\Delta\theta/\Delta\theta_c$ and the external coupling value $T_a = \sqrt{1 - |\Gamma_{\rm A}|^2}$;
- for a given pair of T_a and $\Delta\theta/\Delta\theta_c$ the enforcement of the equiripple condition allows to determine the central coupling value $T_b = |S_{21}^{(b)}|$.

With the help of these properties, the universal equiripple design charts of Fig. 6 were obtained. Hence, the following design scheme was established:

- for a given value of the ripple in the passband, the ratio $\Delta\theta/\Delta\theta_c$ is determined [see Fig. 6(a)];
- the external coupling value T_a is obtained by the contour plot of Fig. 6(b) from the knowledge of the ratio $\Delta\theta/\Delta\theta_c$ determined in the previous step and of the required fractional bandwidth B_θ obtained by (13);
- the central coupling (T_b) is obtained by the chart of Fig. 6(c) from the values of T_a and $\Delta\theta/\Delta\theta_c$ previously determined;
- $\Delta\theta_c$ is evaluated by means of (6);
- the cavity dimensions are determined by means of (5) and (12).

At this point the electrical design of the filter is completed and the coupling discontinuities are defined by means of the magnitude of their transmission coefficients S_{21} at the central frequency and the phase-matching condition (16). The final step is the definition of the geometry of these discontinuities.

The electromagnetic characterization of this kind of discontinuities can be efficiently done by a full-wave technique based on the well-known method of moments [12]. Similar

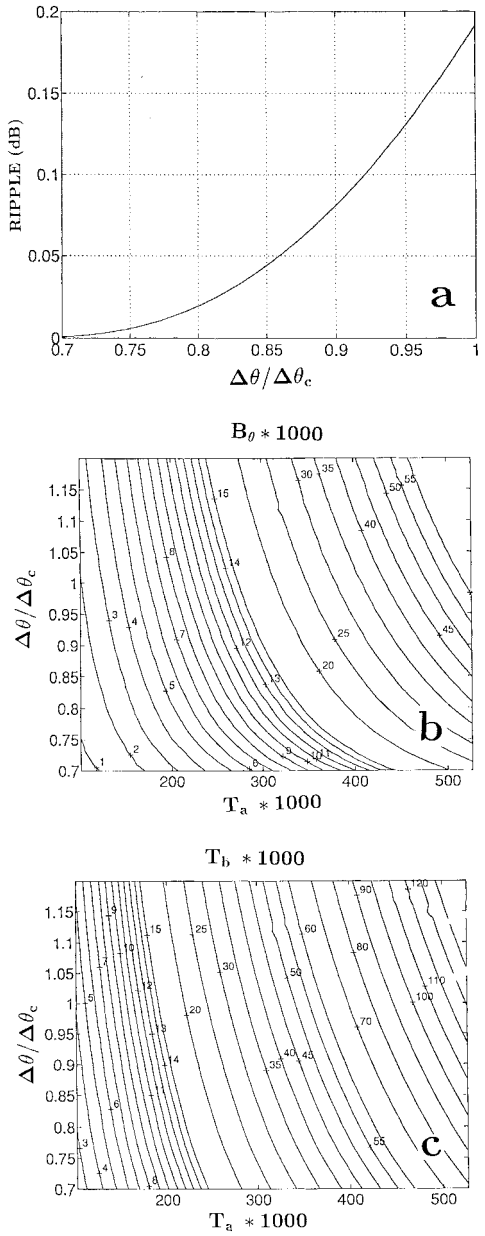

Fig. 6. Equiripple design charts for the dual-mode two-cavity filter. See the text for their use.

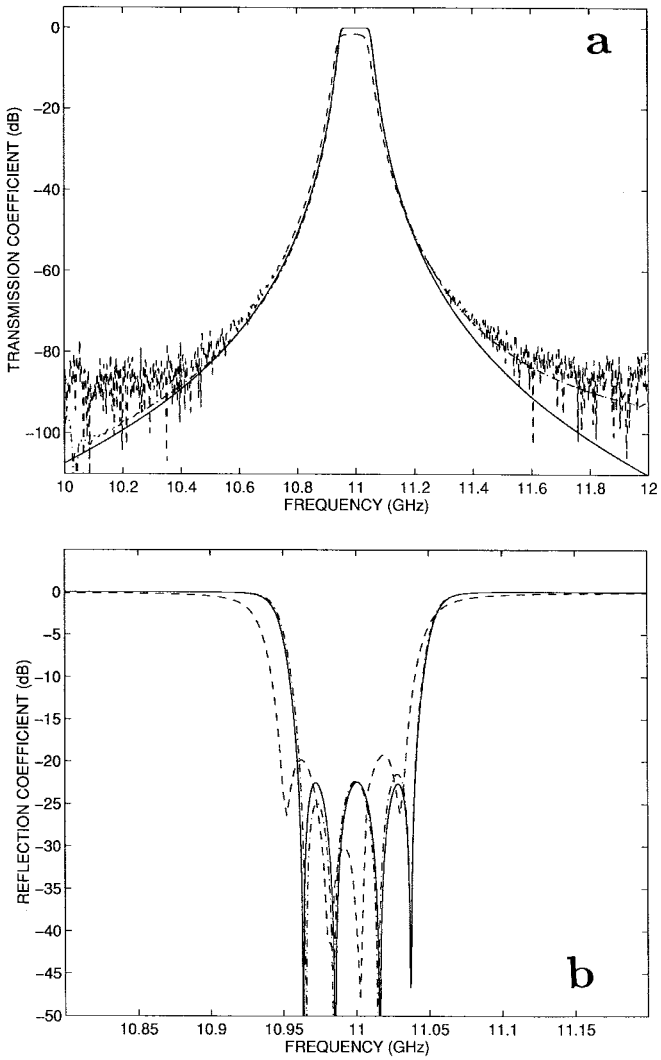

Fig. 7. Frequency response of the dual-mode two-cavity filter. (a) Transmission coefficient. (b) Reflection coefficient. Design (solid line), measured data (dashed line), full-wave analysis (dash-dotted line).

techniques such as the mode matching method can also be applied [13]. The slot thickness can be used to obtain small coupling values without reducing the slot aperture to too small of a size [13]. A possible approach is to view the discontinuity as a cascade of two steps, the generalized scattering matrices of which are computed and combined. This technique is particularly efficient when only the first few modes of the below cut-off waveguide play a role in the interaction between the two opposite faces of the discontinuity. Conversely, for small thicknesses, the cascade procedure becomes burdensome, and it is more convenient to deal with the problem by considering the electric field distributions at both sides of the discontinuity as primary unknowns to be represented in the moment method application [14]. A peculiarity of these discontinuities is the 45° rotation of the apertures with respect to the cavity walls. As reported in [15], this rotation neither introduces significant difficulties nor reduces the reliability of the prediction with respect to the case where the aperture is not inclined.

IV. Design and Results

As an example, we designed and realized a four-pole filter in a WR90 waveguide. The specifications were: central frequency 11 GHz, bandwidth 72 MHz, return loss of 22 dB. The electrical design, carried out according to the procedure presented in Section III, directly gives the frequency response of Fig. 7. Here the discontinuities are represented by frequency-independent scattering matrices, whereas the dual-mode coupling is described rigorously. The unperturbed waveguide has a cross section of 18 × 18 mm. The geometry of the whole filter has been defined as follows. We realized both coupling discontinuities by means of 1 mm thick slots with rectangular apertures. In particular, the central discontinuity has a narrow aperture with a height of 1 mm so that the diagonal modes 1 and 4 are not coupled (see Fig. 4). Notice that if two transmission zeros are required, the aperture height

Fig. 8. Parts of the waveguide filter prototype.

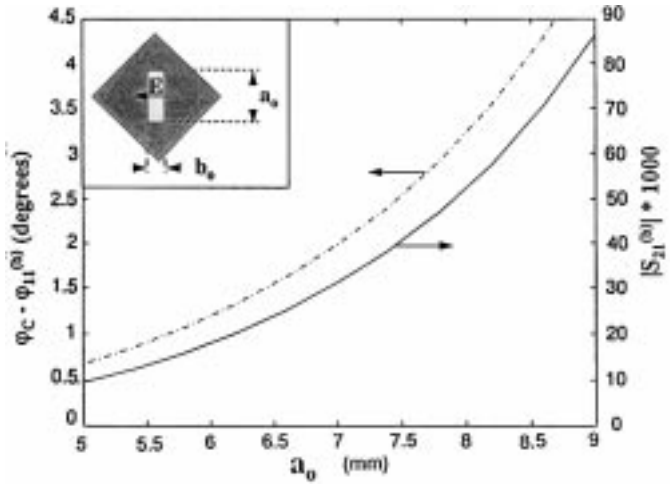

Fig. 9. One-mm-thick central slot in 18×18 mm waveguide; aperture height $b_0 = 1$. mm. $\phi_C - \phi_{11}^{(b)}$ and $|S_{21}^{(b)}|$ against the aperture length a_0 at 11 GHz.

must be increased and the second cavity must be rotated by 90° in order to obtain the desired sign for the coupling between these two modes.

Recalling that the discontinuities must satisfy the phase-matching condition (16), it is convenient at first to define the geometry of the central slot by choosing the aperture length which gives the desired value T_b for the parameter $|S_{21}^{(b)}|$. Fig. 8 shows the influence of the aperture length on this transmission coefficient at 11 GHz. The phase difference $(\phi_C - \phi_{11}^{(b)})$ of the scattering parameters S_{11} corresponding to the diagonal mode 1 and 2, respectively, must also be determined (see Fig. 8 for its typical behavior). Remember that this phase difference must be maintained by the input/output discontinuity. Now, the aperture dimensions of this last discontinuity are obtained by the intersection of two curves selected from the two contour plots of Fig. 9. These contour plots give the magnitude of the transmission coefficient $S_{21}^{(a)}$ and the difference between the phases of the two reflection coefficients $(\phi_B - \phi_A)$ as a function of the aperture dimensions.

The frequency response of the filter obtained by a full-wave analysis is also reported in Fig. 7 (dashed–dotted line). The

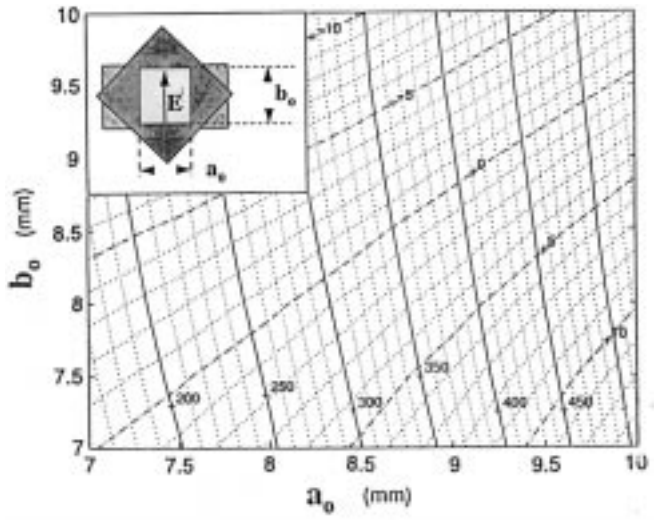

Fig. 10. One-mm-thick input/output slot connecting WR90 and 18×18 mm waveguide. Contour plots of $|S_{21}^{(a)}|$ (solid line, nat*1000) and $\phi_B - \phi_A$ (dotted line, degree) as functions of the aperture dimensions at 11 GHz

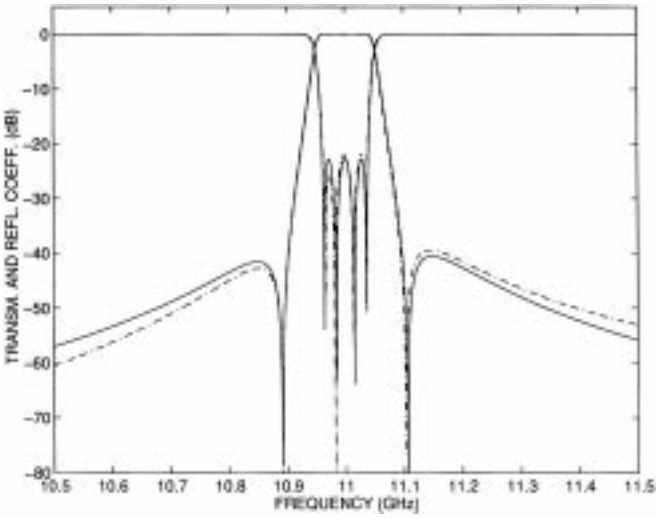

Fig. 11. Frequency response of the dual-mode two-cavity filter with two transmission zeros. Design (solid line), full-wave analysis (dash-dotted line).

width, height and length of the cavities are $18.111 \times 17.899 \times 19.814$ mm. All the aperture dimensions of the slots were chosen to realize the scattering parameters directly obtained by the design procedure and no optimization scheme was applied. The input/output apertures dimensions are 8.725×8.060 mm, while the central aperture is 7.443×1 mm.

The slight difference between the electrical design and the full-wave analysis is related to the frequency dependence of the coupling discontinuities and to the spurious coupling caused by the slots. In fact, since the cross section of the cavity is not rigorously square, weak spurious couplings are generated at the discontinuity sections. However, if the equiripple condition must be satisfied exactly, a design which presents a slope in the ripple envelope can be produced exploiting the geometrical interpretation given in Fig. 5. A prototype, whose parts are shown in Fig. 10, was manufactured and measured, and its frequency response is also reported in Fig. 7. We can observe a rather significant insertion loss in

the passband and a slight lowering of the central frequency. Notice, however, that the prototype is not silver-plated and the tolerances of the sample are larger than those required for filters with very narrow passband like this one. Hence, a better accuracy in the realization of the filter will undoubtedly yield an excellent agreement between the measured and predicted results.

Fig. 11 shows the capability to obtain frequency responses of elliptic function filters with this configuration. Obviously, in this case the diagonal modes 1 and 4 are coupled to each other and the second cavity is rotated by 90° with respect to the first one, so that two transmission zeros appear. The solid line refers to the result obtained directly with the design where the discontinuities are described in terms of frequency independent scattering matrices whereas the dotted line is the result of the full-wave analysis. The synthesis procedure still holds also in this case; obviously, we have to deal with a further input parameter which can be identified as the ratio between the separation of the two transmission zeros and the central frequency.

V. Conclusion

The results presented in this paper show the possibility to realize a dual-mode rectangular waveguide filter with a distributed modal coupling obtained without any discontinuities inside the resonators. This has been possible by exciting the diagonal polarizations of an almost square waveguide. Moreover, all the discontinuities have been realized by thick rectangular slots. A new design scheme based on modal circuits has also been presented and discussed. The use of a distributed model in the synthesis procedure allows for obtaining results closer to the analysis; hence, optimization schemes can be avoided. Comparisons with experimental results have confirmed the validity of this new filter concept. Finally, the point of view used in this paper allows for a deeper insight into the role played by the various parameters involved in the design. In fact, thanks to the geometrical interpretation of the synthesis procedure given in Fig. 5, not only narrow-band filters can be designed. The dispersion of the parameters occurring in the case of broad-band filters generally destroys the equiripple condition and produces a frequency shift. According to this geometrical interpretation, these degradations can be seen as a shift of the intersections between the $\Gamma_D(\theta)$ curve and the circumference corresponding to the central device. Hence, they can be compensated by moving the circumference or the curve $\Gamma_D(\theta)$ that is changing the values of the scattering parameters of the discontinuities.

Acknowledgment

The authors would like to thank M. Bruno and A. Tomasi for the prototype manufacturing. A. Olivieri is gratefully acknowledged for his substantial contribution to measurements.

References

[1] C. Kudsia, R. Cameron, and W. C. Tang, ''Innovations in microwave filters and multiplexing networks for communications satellite systems,'' *IEEE Trans. Microwave Theory Tech.*, vol. 40, pp. 1133–1149, June 1992.

[2] A. E. Williams, ''A four-cavity elliptic waveguide filter,'' *IEEE Trans. Microwave Theory Tech.*, vol. MTT-18, pp. 1109–1113, Dec. 1970.

[3] A. E. Atia and A. E. Williams, ''Narrow-bandpass waveguide filters,'' *IEEE Trans. Microwave Theory Tech.*, vol. MTT-20, pp. 258–265, Apr. 1972.

[4] R. Levy and S. B. Cohn, ''A history of microwave filter research, design, and development,'' *IEEE Trans. Microwave Theory Tech.*, vol. MTT-32, pp. 1055–1067, Sept. 1984.

[5] M. Guglielmi, R. Molina, and A. Melcon, ''Dual-mode circular waveguide filters without tuning screw,'' *IEEE Microwave Guided Wave Lett.*, vol. 2, pp. 457–458, Nov. 1992.

[6] J. F. Liang, X. P. Liang, K. A. Zaki, and A. E. Atia, ''Dual-mode dielectric or air-filled rectangular waveguide filters,'' *IEEE Trans. Microwave Theory Tech.*, vol. 42, pp. 1330–1336, July 1994.

[7] R. Beyer and F. Arndt, ''Efficient modal analysis of waveguide filters including the orthogonal mode coupling elements by a mm/fe method,'' *IEEE Trans. Microwave Theory Tech.*, vol. 5, pp. 9–11, Jan. 1995.

[8] X. Liang, K. A. Zaki, and A. I. Atia, ''Dual-mode coupling by square corner cut in resonators and filters,'' *IEEE Microwave Guided Wave Lett.*, vol. 40, pp. 2294–2302, Dec. 1992.

[9] R. Levy, ''The relationship between dual-mode cavity cross-coupling and waveguide polarizers,'' *IEEE Trans. Microwave Theory Tech.*, vol. 43, pp. 2614–2620, Nov. 1995.

[10] R. Orta, P. Savi, R. Tascone, and D. Trinchero, ''Rectangular waveguide dual-mode filters without discontinuities inside the resonators,'' *IEEE Microwave Guided Wave Lett.*, vol. 5, pp. 302–304, Sept. 1995.

[11] C. Vassallo, *Opt. Waveguide Concepts.* Amsterdam, The Netherlands: Elsevier, 1991, sec. 1.4.

[12] H. Auda and R. F. Harrington, ''A moment solution for waveguide junction problem,'' *IEEE Trans. Microwave Theory Tech.*, vol. MTT-41, pp. 515–519, July 1983.

[13] H. Chang and K. A. Zaki, ''Evanescent-mode coupling of dual-mode rectangular waveguide filters,'' *IEEE Trans. Microwave Theory Tech.*, vol. 39, pp. 1307–1312, Aug. 1991.

[14] R. Pons and D. Pozar, ''A frequency-selective surface using aperture-coupled microstrip patches,'' *IEEE Trans. Antennas Propagat.*, vol. 39, pp. 1763–1769, Dec. 1991.

[15] R. Yang and A. S. Omar, ''Analysis of thin inclined rectangular aperture with arbitrary location in rectangular waveguide,'' *IEEE Trans. Microwave Theory Tech.*, vol. 41, pp. 1461–1463, Aug. 1993.

Patrizia Savi received the Laurea degree in electronic engineering from the Politecnico di Torino, Torino, Italy, in 1985.

In 1986 she worked on the analysis and design of dielectric radomes at Alenia (Caselle Torinese), Torino, Italy. Since 1987 she has worked as a Researcher at CESPA (Centro Studi Propagazione e Antenne) of the Italian National Research Council (CNR), Politecnico di Torino, Torino, Italy. Her research interests are in the area of dielectric radomes, frequency selective surfaces, radar cross sections, waveguide discontinuities, and microwave filters.

Daniele Trinchero was born in Torino, Italy, in 1968. He received the Laurea degree in electronic engineering in 1993 from the Politecnico di Torino, Torino, Italy, and began his Ph.D. studies there in 1994.

In 1996 he worked on the design of frequently selective surface (FSS) antennas as a Visiting Researcher at the Loughborough University of Technology, Leics., U.K. His research interests are in the areas of frequency selective surfaces, waveguide discontinuities, and microwave filters.

Riccardo Tascone was born in Genova, Italy, in 1955. In 1980 he earned the Laurea degree in electronic engineering from the Politecnico di Torino, Torino, Italy.

From 1980 to 1982, he worked at CSELT (Centro Studi e Laboratori Telecomunicazioni, Torino, Italy), where his research has mainly dealt with frequency selective surfaces, waveguide discontinuities, and microwave antennas. He joined CESPA (Centro Studi Propagazione e Antenne, Torino) of the Italian National Research Council (CNR), Politecnico di Torino, Torino, Italy, in 1982 and has held various teaching positions in the area of electromagnetics. He is presently working there as a Senior Scientist (Dirigente di Ricerca). His research interests are in the areas of microwave antennas, dielectric radomes, frequency selective surfaces, radar cross section, waveguide discontinuities, microwave filters, and optical passive devices.

Mr. Tascone is a Member of the Scientific Board at Politecnico di Torino.

Renato Orta (M'93) received the Laurea degree in Electronic Engineering in 1974 from the Politecnico di Torino, Torino, Italy.

Since 1974 he has worked as a member of the Department of Electronics, Politecnico di Torino, Torino, Italy; first as an Assistant Professor, and since 1987 as an Associate Professor. In 1985 he spent one year as a Research Fellow at the European Space Research and Technology Center (ESTEC-ESA) at Noordwijk, The Netherlands. He currently teaches a course on electromagnetic field theory and another on optical components. His research interests include the areas of radiation and scattering, numerical techniques, and microwave and optical components.